PTEN Is a Negative Regulator of NK Cell Cytolytic Function

Edward L. Briercheck,* Rossana Trotta,[†,‡] Li Chen,[†] Alex S. Hartlage,* Jordan P. Cole,[†] Tyler D. Cole,[†] Charlene Mao,[†] Pinaki P. Banerjee,[§,¶] Hsiang-Ting Hsu,[§] Emily M. Mace,[§] David Ciarlariello,[‖] Bethany L. Mundy-Bosse,[†] Isabel Garcia-Cao,[#] Steven D. Scoville,* Lianbo Yu, Robert Pilarski,[††] William E. Carson, III,*[,†,‡‡] Gustavo Leone,*[,†,§§,¶¶] Pier Paolo Pandolfi,[‖,#] Jianhua Yu,[‖‖] Jordan S. Orange,[§,¶] and Michael A. Caligiuri*[,†,¶¶,‖‖]**

Human NK cells are characterized by their ability to initiate an immediate and direct cytolytic response to virally infected or malignantly transformed cells. Within human peripheral blood, the more mature CD56^{dim} NK cell efficiently kills malignant targets at rest, whereas the less mature CD56^{bright} NK cells cannot. In this study, we show that resting CD56^{bright} NK cells express significantly more phosphatase and tensin homolog deleted on chromosome 10 (PTEN) protein when compared with CD56^{dim} NK cells. Consistent with this, forced overexpression of PTEN in NK cells resulted in decreased cytolytic activity, and loss of PTEN in CD56^{bright} NK cells resulted in elevated cytolytic activity. Comparable studies in mice showed PTEN overexpression did not alter NK cell development or NK cell–activating and inhibitory receptor expression yet, as in humans, did decrease expression of downstream NK activation targets MAPK and AKT during early cytolysis of tumor target cells. Confocal microscopy revealed that PTEN overexpression disrupts the NK cell's ability to organize immunological synapse components including decreases in actin accumulation, polarization of the microtubule organizing center, and the convergence of cytolytic granules. In summary, our data suggest that PTEN normally works to limit the NK cell's PI3K/AKT and MAPK pathway activation and the consequent mobilization of cytolytic mediators toward the target cell and suggest that PTEN is among the active regulatory components prior to human NK cells transitioning from the noncytolytic CD56^{bright} NK cell to the cytolytic CD56^{dim} NK cells. ***The Journal of Immunology*****, 2015, 194: 1832–1840.**

Human NK cells are CD56^{+}CD3^{-} large granular lymphocytes of the innate immune system, which are characterized by the ability to both directly kill and initiate an immune response to virally infected or malignantly transformed cells (1). In human blood, NK cells can be divided into two developmentally and functionally distinct subsets based upon cell-surface expression of CD56. In contrast to the more mature CD56^{dim} NK cell, the less mature CD56^{bright} NK cell is unable to efficiently kill malignant cells at rest (2). The molecular mechanisms underlying this difference are incompletely defined.

In order for NK cells to carry out an effective yet controlled response, NK cell activation is mediated by a dynamic integration of signaling through activating and inhibitory receptors on the NK cell surface, which, in turn, are regulated by kinases and phosphatases, respectively. Further, in the case of cytotoxicity mediated by the release of lytic granules, the NK cell must integrate these signals to execute the proper directional secretion of the granules onto the target cell (3). Previous reports have demonstrated the importance of the PI3K/AKT and MAPK pathways for regulating NK cell cytolytic activity (4–7). Additionally, in human NK cells, the 5′-lipid phosphatase SHIP-1 is a negative regulator of PI3K/AKT and MAPK, and high SHIP-1 expression correlates with decreased NK cell natural cytotoxicity and IFN-γ production (8).

The 3′-lipid phosphatase called phosphatase and tensin homolog deleted on chromosome 10 (PTEN) is a critical tumor sup-

*Medical Scientist Training Program and Biomedical Sciences Graduate Program, The Ohio State University, Columbus, OH 43210; [†]The Comprehensive Cancer Center and Arthur G. James Cancer Hospital and Richard J. Solove Research Institute, The Ohio State University, Columbus, OH 43210; [‡]Department of Microbiology and Immunology and Marlene and Stewart Greenebaum Cancer Center, University of Maryland School of Medicine, Baltimore, MD 21201; [§]Center for Human Immunobiology, Baylor College of Medicine Texas Children's Hospital, Baylor College of Medicine, Houston, TX 77030; [¶]Department of Pediatrics, Baylor College of Medicine Texas Children's Hospital, Houston, TX 77030; [‖]The Molecular, Cellular, and Developmental Biology Program, The Ohio State University, Columbus, OH 43210; [#]Cancer Genetics Program, Beth Israel Deaconess Cancer Center, Department of Medicine and Pathology, Beth Israel Deaconess Medical Center, Harvard Medical School, Boston, MA 02215; **Center for Biostatistics, The Ohio State University, Columbus, OH 43210; [††]Division of Human Genetics, Department of Internal Medicine, The Ohio State University, Columbus, OH 43210; [‡‡]Department of Surgery, The Ohio State University, Columbus, OH 43210; [§§]Department of Molecular Genetics, The Ohio State University, Columbus, OH 43210; [¶¶]Department of Molecular Virology, Immunology, and Medical Genetics, The Ohio State University, Columbus, OH 43210; and [‖‖]Division of Hematology, Department of Internal Medicine, The Ohio State University, Columbus, OH 43210

Received for publication May 13, 2014. Accepted for publication December 5, 2014.

This work was supported by National Cancer Institute Grants CA16058 (to M.A.C.), CA95426 (to M.A.C.), and CA68458 (to M.A.C.). E.L.B. is supported by the Pelotonia Fellowship Program (Columbus, OH). B.L.M.-B. is supported by National Institutes of Health Training Grant T32-CA009338 (to M.A.C).

E.L.B. designed the study, performed research work, analyzed data, and wrote the manuscript; R.T. contributed to the design of the study and writing and editing of the manuscript; L.C., A.S.H., J.P.C., T.D.C., D.C., B.L.M.-B., R.P., and S.D.S. performed experimental work; C.M., P.P.B., E.M.M., and H.-T.H. performed experimental work and analyzed data; I.G.-C. and P.P.P. developed the Super-PTEN transgenic mice and reviewed and edited the manuscript; L.Y. provided statistical analyses; and W.E.C., G.L., J.Y., J.S.O., and M.A.C. contributed to the design of the study and writing and editing of the manuscript.

Address correspondence and reprint requests to Dr. Michael A. Caligiuri, The Ohio State University Comprehensive Cancer Center, 460 West 12th Avenue, Columbus, OH 43210. E-mail address: michael.caligiuri@osumc.edu

Abbreviations used in this article: miR, microRNA; MTOC, microtubule organizing center; PTEN, phosphatase and tensin homolog deleted on chromosome 10; shPTEN, short hairpin RNA–targeting phosphatase and tensin homolog deleted on chromosome 10; WT, wild-type.

pressor for which mutations and/or deletions occur in and are associated with a wide variety of cancers (9). Additionally, inherited mutations of PTEN encompass a clinical spectrum of disorders referred to as PTEN hamartoma tumor syndromes, including Cowden syndrome, Bannayan-Riley-Ruvalcalba syndrome, *Proteus* syndrome, and *Proteus*-like syndrome (10).

A major mechanism of PTEN-mediated tumor suppression has been attributed to its function as a lipid phosphatase inhibitor of the PI3K/AKT pathway; however, PTEN has proven to be a complex regulator of cellular homeostasis with both lipid phosphatase–dependent and –independent roles in proliferation, senescence, motility, and chromosomal stability (11–20). Recently, PTEN has also emerged as an important regulator of immune function. Loss of Pten in T cells can lead to variable consequences ranging from a lethal autoimmunity to enhancement or deficiency in tumor immunity depending upon the developmental timing and the specific T cell subset in which PTEN is deleted (21–26). To our knowledge, a role for PTEN in regulating NK cell immune function has not been investigated. In this report, we provide an investigation of PTEN expression and function in human and mouse NK cells and assess its role in the regulation of cytotoxicity against leukemic target cells.

Materials and Methods

NK cell preparations

Human and murine NK cells were isolated and cultured as described (27, 28). All human work was approved by the Institutional Review Board of The Ohio State University. All animal work was approved by The Ohio State University Animal Care and Use Committee.

Immunoblot

Immunoblots were run as described (29). Abs used were: rabbit monoclonal anti-PTEN, anti–phospho-AKT^{Ser473}, anti–phospho-ERK$^{Thr202/Tyr204}$ (Cell Signaling Technology), and mouse anti-GRB2 Ab (BD Pharmingen). Densitometry was determined using ImageJ software (National Institutes of Health). The area gated in compared samples was determined by the largest visible band in each developed film. Relative protein of interest levels were then normalized to loading controls, and ratios were calculated as the difference between these values.

Real-time PCR

Total RNAs were extracted from 20,000–40,000 cells/sample using RNeasy Mini Kit (catalog number 74106; Qiagen). First-strand cDNAs were synthesized using SuperScript VILO Master Mix (catalog number 11755250; Invitrogen). Data were analyzed using the comparative δ-δ threshold cycle method and normalized to 18sRNA for loading controls. Results (mean ± SD of triplicate wells) are represented as fold changes of expression levels.

Confocal microscopy

Normal donor NK cells were enriched with RosetteSep (StemCell Technologies), incubated on anti-CD18 and anti-CD56 Ab-coated glass slides at 37°C for 30 min, and then permeabilized and stained intracellularly as described (30). F-actin was detected with Phalloidin Alexa Fluor 568 (Life Technologies) and perforin with anti-perforin FITC (BD Pharmingen). PTEN was detected by anti-PTEN mAb (Thermo Scientific) followed by Alexa Fluor 647 goat anti-mouse Ab (Life Technology). Coverslips were mounted with Vectashield (Vector Laboratories).

Mice

Super-PTEN transgenic mice (C57BL/6J) have been described (31).

Plasmids

PTEN cDNAs were cloned into a pCDH-EF1-MCS-T2A-copGFP vector (System Biosciences). PTEN cDNA was cloned out of a pCMV6-XL5 vector (Origene). PTEN cDNA with a mutation in the lipid phosphatase catalytic site (G129E) was cloned out of a published vector [Addgene plasmid 30377 (32)]. A short-hairpin sequence targeting PTEN was cloned into PSIH1-H1-copGFP vector (System Biosciences).

Cells lines

The human IL-2–dependent NK cell line NK-92 (ATCC CRL-2407; American Type Culture Collection) was maintained in culture in RPMI 1640 medium supplemented with 20% heat-inactivated FBS (Invitrogen), 2 mM L-glutamine, and 150 IU/ml recombinant human IL-2 (Hoffman-LaRoche). The YAC-1 mouse T-lymphoma cell line and human erythroleukemia cell line K562 (American Type Culture Collection) were maintained in RPMI 1640 supplemented with 10% heat-inactivated FBS and 2 mM L-glutamine. The amphotropic-packaging cell line 293T (American Type Culture Collection) was maintained in culture in DMEM/10% FBS medium and grown for 16–18 h to 80% confluence prior to transfection by calcium phosphate–DNA precipitation (Profection system; Promega).

Lentiviral infections

293T packaging cells were seeded onto a 15-cm dish (catalog number 430599; Corning) at 5 to 6 × 10^6/40 ml/dish. Cells reaching 80–90% confluence 40–48 h later were used for cotransfection. Media were switched to 40 ml fresh D10F with chloroquine (25 μM at final) before cotransfection to assemble lentiviruses. Three plasmids were used to prepare DNA precipitates. These included the control or experimental construct (100 μg) and the packaging plasmids VSVG (50 μg) and deltaR9 (150 μg). The plasmids were diluted with 1x TE (pH 8) to a final volume of 1.0125 ml, and then 112.5 μl 2 M $CaCl_2$ was added and mixed. An equal volume of 1.125 ml 2x HBS buffer (50 mM HEPES, 280 mM NaCI, 12 mM dextrose, 10 mM KCI, and 1.5 mM Na_2PO_4 [pH 7.05]) was added to the mixture. The whole mixture was quickly vortexed for 30–45 s and then added to the top of the media immediately without disturbing the single cell layer. Cells were cultured in a 37°C incubator supplied with 3% CO_2. After overnight media was removed and 40 ml fresh D10F was added, cells were cultured in a 37°C incubator with 5% CO_2, and sodium butyrate was added at a final concentration of 1 mM. Viral supernatants were harvested twice at 24 and 48 h after adding sodium butyrate, respectively. The 24- and 48-h supernatants were merged and passed through 0.45-um size filter after spinning at 2000 rpm for 5 min. Filtered viral supernatants were centrifuged at 16,500 rpm for 90 min at 4°C. After centrifugation, supernatants were removed, and fresh supernatants containing virus were added to the same tubes containing virus pellets from the previous round. Three to four rounds of successive ultracentrifugation were performed and resuspended in 900–1000 μl 1x PBS overnight at 4°C and transferred to −80°C until use. For primary experiments, human primary NK cells were enriched from leukopacks using the RosetteSep kit (catalog number 15065; StemCell Technologies) following the manufacture's protocol with 60–70% purity. NK subsets were sorted from enriched NK cells using the FACSAria II sorter (BD Biosciences) with a typical purity >98 to 99% and a total number of 1.0–1.6 × 10^6 cells/donor were obtained after sorting. Sorted bright NK cells were cultured at 0.5–0.8 × 10^6 cells/200 μl/well in 96-well plate (round bottom) with RPMI 1640 containing 10% FBS and 5% glutamate (R10F), together with 450 U/ml IL-2. After overnight culture, 180 μl media was removed following spinning of the plate at 2000 rpm for 5 min at room temperature, and 100 μl concentrated viruses were added to each well, together with an equal volume of RPMI 1640 containing 20% FBS, 900 U/ml IL-2, and 16 μg/ml polybrene. The cells were mixed well with viruses and cultured for 1 h in a 37°C incubator supplied with 5% CO_2, followed by spinning in a microcarrier bucket at 2000 rpm for 2 h at 20–25°C. This infection procedure of 1-h culture plus 2-h spin was repeated three times. Before each round of adding new viruses, all supernatants were collected and transferred to a six-well plate. After the last spin, cells including all supernatants were transferred to a six-well plate and merged with previous supernatants. Fresh media (R10F) containing 450 U/ml IL-2 was then added to a final of volume of 6 ml/well. A total multiplicity of infection of 4–10 was used for transduction. Infected NK cells were cultured for 3 d postinfection, then stained with allophycocyanin CD56 and FITC-CD3e before sorting for $GFP^+CD56^+CD3^-$ NK cells. As a control, sorted NK cells with mock infection were used for gating GFP-positive cells. Sorted $GFP^+CD56^+CD3^-$ cells were typically 80–90% pure and gave a yield of 0.1–0.3 × 10^6 cells/sample. Successful overexpression or knockdown was confirmed by immunoblot.

Abs and flow cytometric analysis

Murine splenocytes were stained with Abs (clones) from BD Biosciences reactive against: NKp46 (29A1.4), NK1.1 (PK136), CD3ε (145-2C11), CD117 (ACK45), CD27 (LG.3A10), CD11b (M1/70), CD49b (DX5), Ly-49C/I (5E6), Ly-49I (YLI-90), Ly-49A (A1), CD16/32 (2.4G2), Ly-49D (4E5), Ly-49G2 (4D11), 2B4 (eBio244F4), NKG2ACE (20d5), and CD69 (H1.2F3). Abs to mouse CD94 (18d3) and NKG2D (CX5) were from

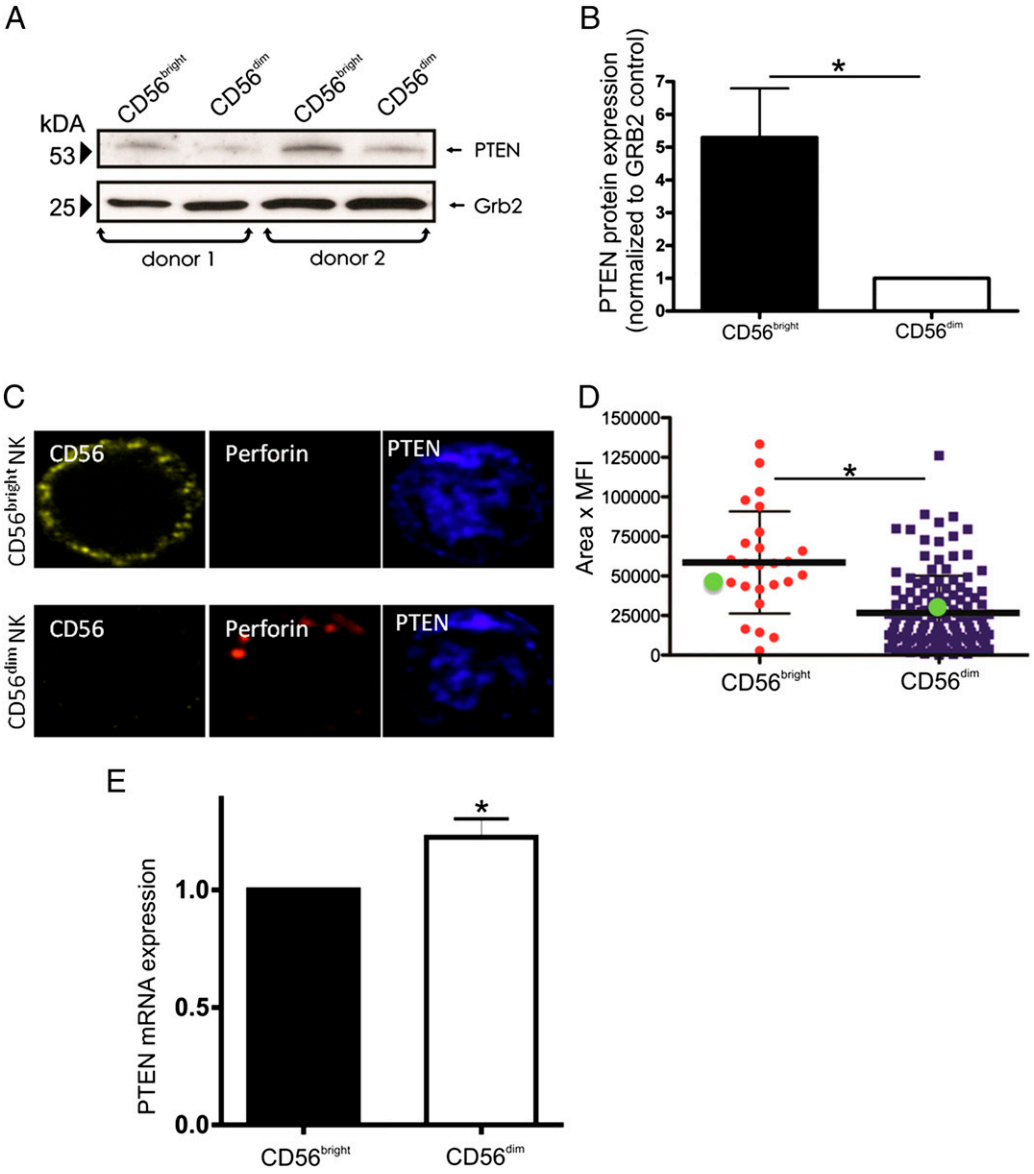

FIGURE 1. PTEN is differentially expressed in human CD56^{bright} versus CD56^{dim} NK cells. NK cells were isolated from the peripheral blood of healthy donors. (**A**) Two representative donor immunoblots showing PTEN protein expression in CD56^{bright} and CD56^{dim} NK cells. GRB2 is shown as a loading control. (**B**) Average PTEN protein expression in CD56^{bright} NK cells (black) relative to CD56^{dim} NK (white) in seven healthy controls. *$p < 0.02$. (**C**) A single plane confocal image (original magnification ×60) of a CD56^{bright} NK cell (*top panel*) and CD56^{dim} NK cell (*bottom panel*) shown stained with CD56 (yellow), perforin (red), and PTEN (blue). (**D**) Mean fluorescence intensity (MFI) × area of PTEN staining in CD56^{bright} and CD56^{dim} NK cells. *$p <$ 0.0001. The green dots in (D) represent the quantitative analysis of the exact image that is shown in (C). Cells were imaged in a single *z*-plane on a Zeiss Axio-Observer Z1 equipped with a Yokogawa CSU10 spinning disc, Zeiss 63× 1.43 NA objective, and Hamamatsu Orca-AG camera. Images were acquired with Volocity software (PerkinElmer). (**E**) PTEN mRNA expression in CD56^{bright} NK cells (black bar) and CD56^{dim} NK cells (white bar; *$p < 0.04$).

eBioscience. NKp46^{+}CD3^{-} cells were gated for FACS analysis of these Ags and analyzed with FlowJo v7.6.1 (Tree Star).

NK cell activation assays

For assessment of NK-92 activation during cytotoxicity with K562 leukemic cells, NK-92 cells were starved from IL-2 for 2 h on ice, then mixed with paraformaldehyde-fixed K562 cells at a 5:1 ratio, and stimulated for the indicated times as described (7). For mice, primary mouse NK cells were expanded in IL-2 for ≥8 d, starved from IL-2 for 2 h on ice, then mixed with paraformaldehyde-fixed YAC-1 lymphoma cells at a 5:1 ratio, and stimulated for the indicated times.

Cytotoxicity assays

For mice, YAC-1 cells were combined with primary mouse NK cells in a standard cytotoxicity assay (7) following NK cell culture in 900 IU/ml IL-2 for 8 d. For humans, K562 leukemic cells were used as targets in a 4-h [^{51}Cr] release assay (7) with empty vector, Over-PTEN, Over-PTEN-G129E, and short hairpin RNA–targeting PTEN (shPTEN)–infected NK-92 and/or primary NK cells that were cultured in 150 IU/ml IL-2.

Immune conjugates assessed by confocal microscopy

Conjugate formation, fixation, and permeabilization were performed as described (33) followed sequentially by: 1) staining with PTEN as described above; or 2) blocking with 10 μg/ml mouse IgG; anti–α tubulin-biotynlated Ab (1:50; Invitrogen); streptavidin–Pacific Blue (1:50; Invitrogen); anti-perforin FITC Ab (1:3; BD Biosciences); and Phalloidin AF-568 (1:100; Invitrogen).

For analysis, a fixed-intensity threshold was used to detect perforin or α-tubulin staining above the background, and the α-tubulin–defined microtubule organizing center (MTOC) was located as described (33). MTOC polarization, granule convergence, and F-actin accumulation were measured as described (34). Although there is spectral overlap between GFP and FITC, the images for Fig. 5 were generated using permeabilized and fixed cells. To avoid any residual GFP overlap with FITC, we

employed single fluorophore controls (GFP-only and FITC-only) to identify a laser power and camera exposure time that adequately detected FITC while not detecting any GFP fluorescence above background.

Statistics

For donor cell data, we calculated ratios between $CD56^{bright}$NK and $CD56^{dim}$NK cells and performed a one-sample *t* test on log-transformed ratios for difference. For cytolytic activity data, we employed an ANOVA model with treatment and target ratio as effects and experiment as block factor. The *t* test was then used for testing treatment differences. Multiplicity was adjusted by Holm's method for significance (35).

Results

PTEN is differentially expressed between human $CD56^{bright}$NK and $CD56^{dim}$NK cells

In contrast to the more mature $CD56^{dim}$ NK cell, $CD56^{bright}$ NK cells are unable to kill malignant targets at rest. We first noted that $CD56^{bright}$ NK cells expressed significantly less microRNA (miR)-26 when compared with $CD56^{dim}$ NK cells ($n = 4$, $p < 0.04$; not shown). Given the role of miR-26 in the regulation of the lipid phosphatase PTEN (36), we hypothesized that a differential expression of PTEN between the two human NK cell subsets could contribute toward this functional difference in cytotoxicity. Immunoblots showed that expression of PTEN protein is increased ~5-fold in $CD56^{bright}$ NK cells compared with $CD56^{dim}$ NK cells (Fig. 1A, 1B, average increase 5.29; $n = 4$, $p < 0.02$; range 2.4–9.4). We confirmed this using confocal microscopy, which showed that NK cells brightest for CD56 also expressed the highest levels of PTEN protein (Fig. 1C, 1D; average 2.2-fold increase in mean fluorescence intensity × area; $p < 0.0001$). To determine whether PTEN is regulated at the translational level, we investigated the expression of PTEN mRNA between the $CD56^{bright}$ and $CD56^{dim}$ NK cell subsets. In contrast to protein expression, PTEN RNA expression was 1.3-fold higher in the $CD56^{dim}$ NK cell subset, suggesting that posttranscriptional regulation accounts for the differences in PTEN protein expression (Fig. 1E; $n = 3$, $p < 0.04$).

PTEN expression negatively correlates with NK cell cytolytic activity

To determine the effect of PTEN expression on NK cell cytolytic activity, we infected the human NK cell line NK-92 with a lentiviral vector encoding either GFP (pCDH-EF1-MCS-T2A-copGFP [empty vector]) or GFP and PTEN (pCDH-EF1-MCS-T2A-copGFP-PTEN [Over-PTEN]) and confirmed PTEN protein overexpression by immunoblot (Fig. 2A). Over-PTEN NK-92 cells showed a significantly decreased efficiency in cytotoxicity against the NK-sensitive leukemic cell line K562 (Fig. 2B; $n = 3$, $p < 0.0001$). To confirm these findings, we infected primary human NK cells isolated from healthy donors with either empty vector or Over-PTEN. We confirmed PTEN expression by immunoblot (Fig. 2C). In agreement with our findings in the NK-92 cell line, primary NK cells overexpressing PTEN demonstrated a significant decrease in cytolytic activity against leukemic target cells (Fig. 2D; $n = 3$, $p < 0.03$). Given our observation that PTEN expression is higher in $CD56^{bright}$ NK cells that have lower cytotoxic activity, we sought to determine if loss of PTEN would increase the cytolytic activity in this population. Therefore, we

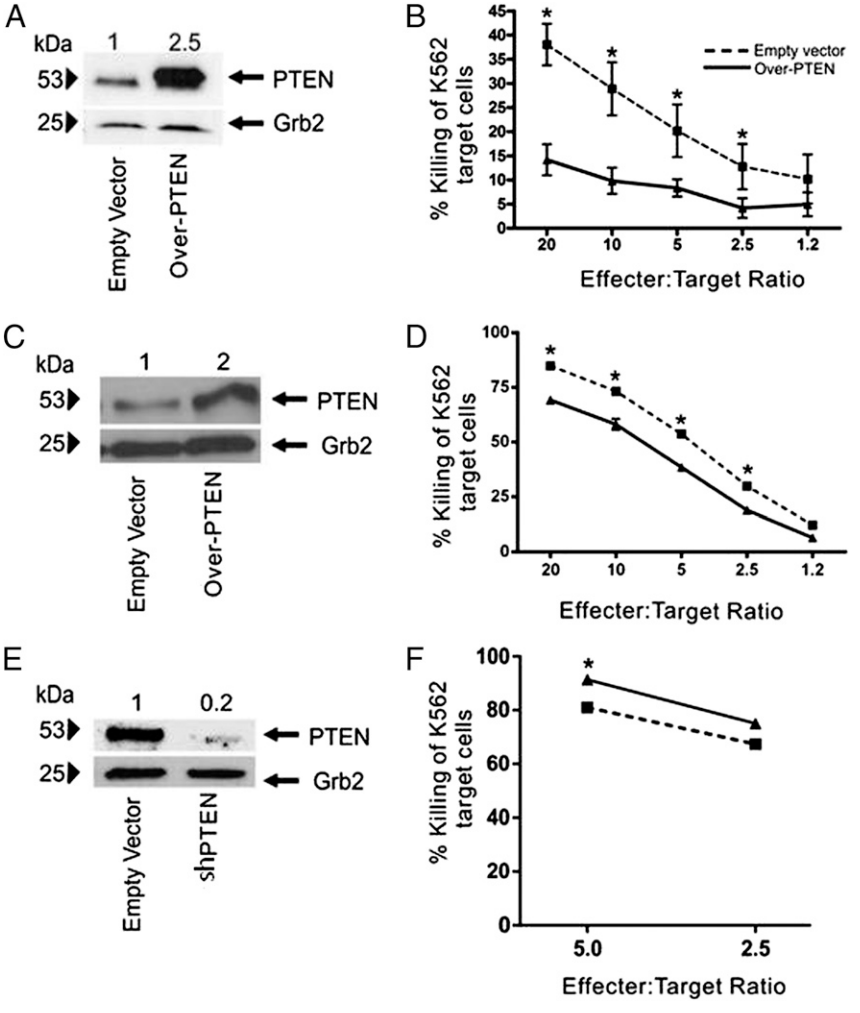

FIGURE 2. PTEN regulates NK cell cytolytic activity. (**A**) Immunoblot of PTEN protein expression in NK cells infected with lentivirus containing cDNA encoding GFP alone (empty vector) or GFP and PTEN (Over-PTEN). Grb2 was used as loading control, with relative densitometry shown above corresponding columns. (**B**) Cytolytic activity of Over-PTEN NK-92 cells (solid line, triangles) versus empty vector (dashed line, squares) against K562 erythroleukemia cells (*$p < 0.0001$). (**C**) Immunoblot of PTEN protein expression in primary NK cells infected with lentivirus containing cDNA encoding GFP alone (empty vector) or GFP and PTEN (Over-PTEN). Grb2 was used as loading control, with relative densitometry shown above corresponding columns. (**D**) Cytolytic activity of Over-PTEN primary human NK cells (solid line, triangles) versus empty vector (dashed line, squares) against K562 erythroleukemia cells (*$p < 0.03$). (**E**) Immunoblot of PTEN protein expression in primary NK cells infected with lentivirus containing cDNA encoding GFP alone (empty vector) or GFP and shPTEN. Grb2 was used as loading control with relative densitometry shown above corresponding columns. (**F**) Cytolytic activity of shPTEN primary human NK cells (solid line, triangles) versus empty vector (dashed line, squares) against K562 erythroleukemia cells in a representative primary donor (*$p < 0.03$).

used a lentiviral vector encoding either GFP (PSIH1-H1-copGFP [empty vector]) or GFP and a short-hairpin RNA targeting PTEN (PSIH1-H1-copGFP-shPTEN [shPTEN]). We confirmed PTEN knock down by immunoblot (Fig. 2E). Loss of PTEN protein led to a significant increase in NK cell cytolytic activity among the less mature $CD56^{bright}$ NK cells (Fig. 2F; $n = 3$, $p < 0.03$), further supporting a role for PTEN in suppressing NK cell cytolytic activity in this subset.

Effect of PTEN overexpression on murine NK cell cytolytic activity and development

To determine whether PTEN regulates murine NK cell cytolytic activity, we isolated $NKp46^{+}CD3^{-}$ NK cells from Super-PTEN transgenic mice (31). We confirmed overexpression of PTEN in Super-PTEN NK cells by immunoblot (Fig. 3A) and then tested their cytotoxicity against the murine NK cell tumor target cell line YAC-1. Super-PTEN NK cells lysed YAC-1 tumor cells with a significantly lower efficiency compared with wild-type (WT) littermate controls (Fig. 3B; $n = 3$, $p < 0.0001$). We next determined if the decreased killing was due to differences in development or expression of NK cell surface receptors. $CD11b^{low}CD27^{low}$, $CD11b^{low}CD27^{high}$, $CD11b^{high}CD27^{high}$, and $CD11b^{high}CD27^{low}$ represent four sequential stages of terminal mouse NK cell maturation (37, 38). After gating on $NKp46^{+}CD3^{-}$ NK cells, we saw no significant change in the proportions of any of the aforementioned populations compared with WT mice, indicating that PTEN overexpression does not disrupt NK cell terminal development (Fig. 3C; $n = 3$, $p = 0.980$). In addition, there were no significant differences in the expression of NK1.1, 2B4, DX5, Ly49H, Ly49D, Ly49A, CD117, CD94, NKG2D, CD27, KLRG1, CD69, CD62L, NK2ACE, and CD16 (Fig. 3D).

Effect of PTEN overexpression on activation of AKT and MAPK

The PI3K/AKT pathway is important for NK cell–mediated cytotoxicity (9), and PTEN regulates the PI3K/AKT pathway. Therefore, we sought to determine if downregulation of PI3K/AKT might account for the decrease in cytolytic activity observed in PTEN-overexpressing NK cells (39). To test this, we stimulated NK-92 cells overexpressing PTEN with fixed K562 target cells for 0, 1, 3, and 10 min and assessed activated AKT. NK-92 cells overexpressing PTEN cells showed a marked reduction in AKT activation during early cytolysis (Fig. 4A). Similarly, Super-PTEN murine NK cells stimulated with Yac-1 target cells also showed a marked reduction in AKT (Fig. 4B). An additional downstream target of PI3K is ERK (MAPK), which is a positive regulator of NK cell cytotoxicity (4, 5, 7). Sustained ERK activation was significantly decreased in both human NK-92 cells overexpressing PTEN and Super-PTEN mouse NK cells compared with respective controls (Fig. 4A, 4B, respectively).

To determine if the negative regulation of NK cell cytolytic activity by PTEN was due to activity at PTEN's lipid phosphatase

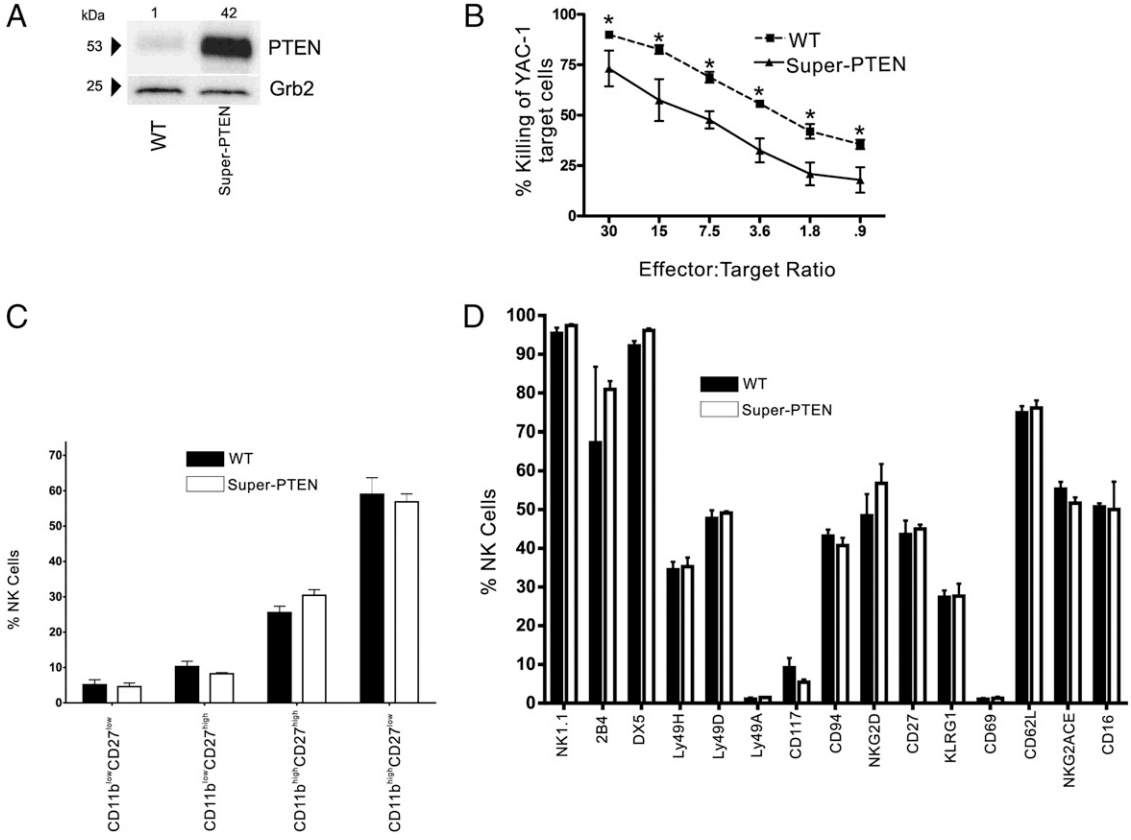

FIGURE 3. PTEN overexpression negatively regulates murine NK cell cytolytic activity but does not affect NK cell development. (**A**) Immunoblot for PTEN protein expression in NK cells isolated from WT littermate controls and Super-PTEN transgenic mice. Grb2 was used as a loading control, with relative densitometry shown above corresponding columns. (**B**) Cytolytic activity of primary NK cells cultured for at least 8 d in IL-2 from Super-PTEN mice (solid line, triangles) versus WT littermate controls (dashed line, squares) against YAC-1 lymphoma cells (*$p < 0.001$). (**C**) Freshly isolated splenocytes from WT littermate controls (black bars) and Super-PTEN mice (white bars) were gated on $NKp46^{+}CD3^{-}$ cells and assessed for percentage of $CD11b^{low}CD27^{low}$, $CD11b^{low}CD27^{high}$, $CD11b^{high}CD27^{high}$, and $CD11b^{high}CD27^{low}$ subsets. (**D**) Splenocytes gated on $NKp46^{+}CD3^{-}$ cells from WT littermate control (black bars) and Super-PTEN mice (white bars) were assessed for their expression of NK cell–activating and inhibitory receptors by flow cytometry.

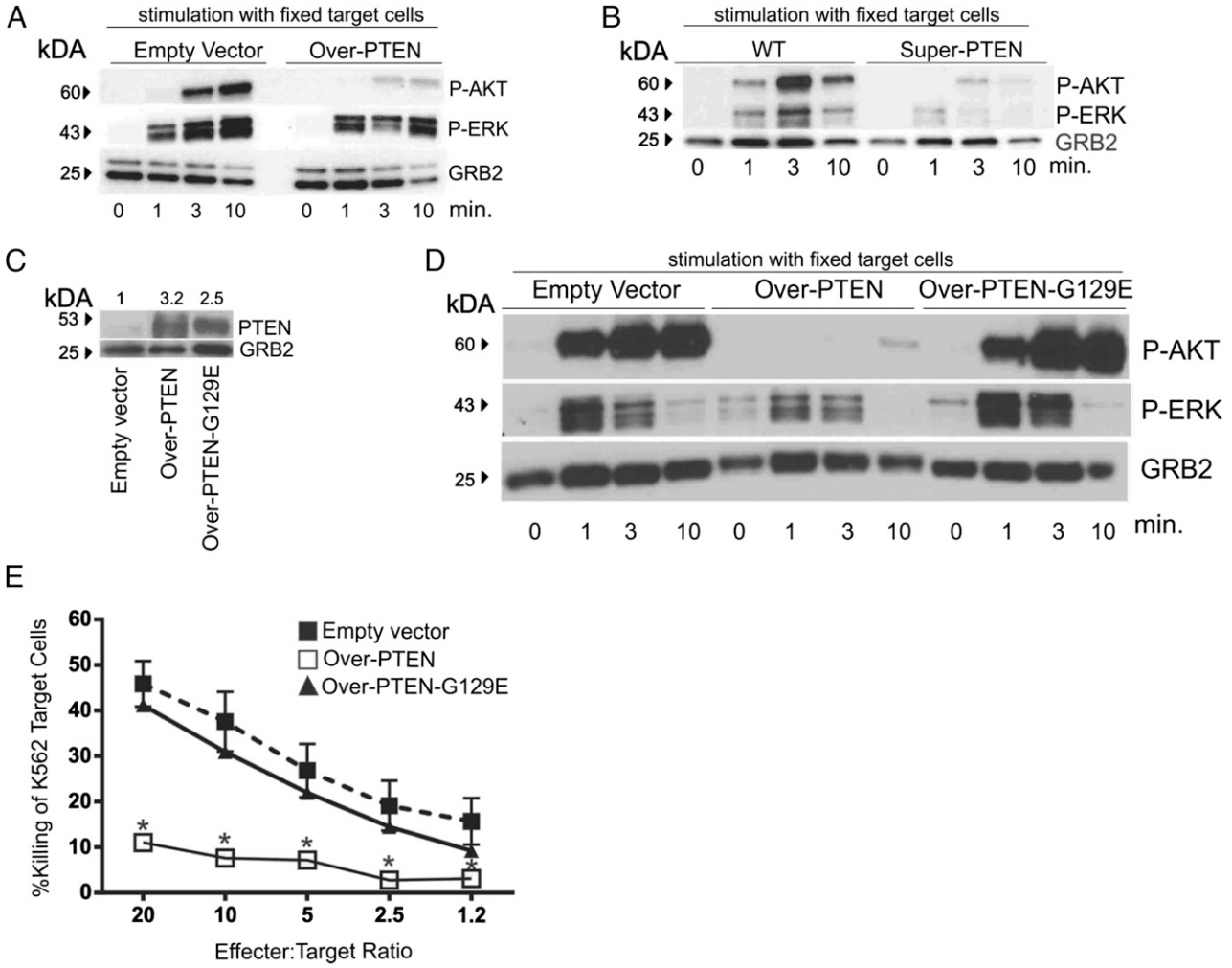

FIGURE 4. PTEN overexpression negatively regulates NK cytolytic activity through inhibition of the AKT and MAPK pathways. (**A**) Immunoblot for p-AKT and p-ERK protein expression in lysates from NK-92 cells infected with empty vector (*left panel*) or Over-PTEN (*right panel*) after stimulation with fixed K562 erythroleukemia cells for 0, 1, 3, and 10 min. (**B**) Immunoblot for p-AKT and p-ERK protein expression in lysates from WT (*left panel*) and Super-PTEN (*right panel*) NK cells after stimulation with fixed YAC-1 target cells for 0, 1, 3, and 10 min. (**C**) Immunoblot for PTEN protein expression in lysates from NK-92 cells infected with lentivirus containing cDNA encoding GFP alone (empty vector), cDNA encoding GFP and WT PTEN (Over-PTEN), or GFP and PTEN with a glycine to glutamate substitution at position 129 (Over-PTEN-G129E). Grb2 was used as a loading control with relative densitometry shown above corresponding columns. (**D**) Immunoblot for p-AKT and p-ERK protein expression from NK-92 cells infected with empty vector (*left panel*), Over-PTEN (*middle panel*), or Over-PTEN-G129E (*right panel*) after stimulation with fixed K562 erythroleukemia cells for 0, 1, 3, and 10 min. (**E**) Cytolytic activity of NK-92 cells infected with Over-PTEN (solid line, open squares) versus empty vector (dashed line, filled squares) versus Over-PTEN-G129E (solid line, triangles), against K562 erythroleukemia cells ($*p < 0.0001$).

catalytic site, we generated an NK-92 cell line that overexpressed PTEN with a glycine to glutamate substitution in position 129 (Over-PTEN-G129E), a mutation known to disrupt PTEN's lipid phosphatase activity (Fig. 4C) (32). This mutation led to a recovery of AKT and ERK activation levels upon stimulation with fixed K562 cells (Fig. 4D), and rescued cytolytic activity to levels not significantly different from empty vector (Fig. 4E).

Effect of PTEN loss on directed granule mobilization

To kill, the NK cell must polarize in response to target binding, and PI3K is crucial in generating directional polarization of NK cells, which in turn is important for E:T cell conjugation (3, 26). We compared NK cell–target cell conjugates between NK-92 cells infected with empty vector and NK-92 cells overexpressing PTEN. NK-92 cells overexpressing PTEN showed decreased polarization of the MTOC (Fig. 5A, 5B; $n \geq 15$, $p < 0.01$) and decreased convergence of lytic granules to the microtubule organizing center (MTOC) (Fig. 5A, 5C; $n \geq 15$, $p < 0.01$). Additionally, NK-92 cells overexpressing PTEN showed significantly decreased F-actin at the immune synapse (Fig. 5A, 5D; $n \geq 15$, $p < 0.01$). Taken together, these data indicate that NK-92 cells overexpressing PTEN have significantly decreased polarization, granule convergence, and F-actin accumulation at the immune synapse compared with NK-92 cells expressing empty vector, suggesting that PTEN does indeed participate in the directional polarization of NK cells following tumor cell conjugation.

Discussion

Certain lipid phosphatases have been shown to be key regulators of NK cell activity against malignant targets; however, the tumor suppressor and lipid phosphatase PTEN had yet to be investigated in NK cells (40). In this report, we use a combination of human and murine studies to assess the role of PTEN in NK cell cytolytic function. We observed that PTEN is more highly expressed in resting noncytolytic $CD56^{bright}$ NK cells than in resting cytolytic $CD56^{dim}$ NK cells, and we therefore hypothesized that the level of PTEN expression in human NK cells could be important in the acquisition and maintenance of NK cell cytolytic function as

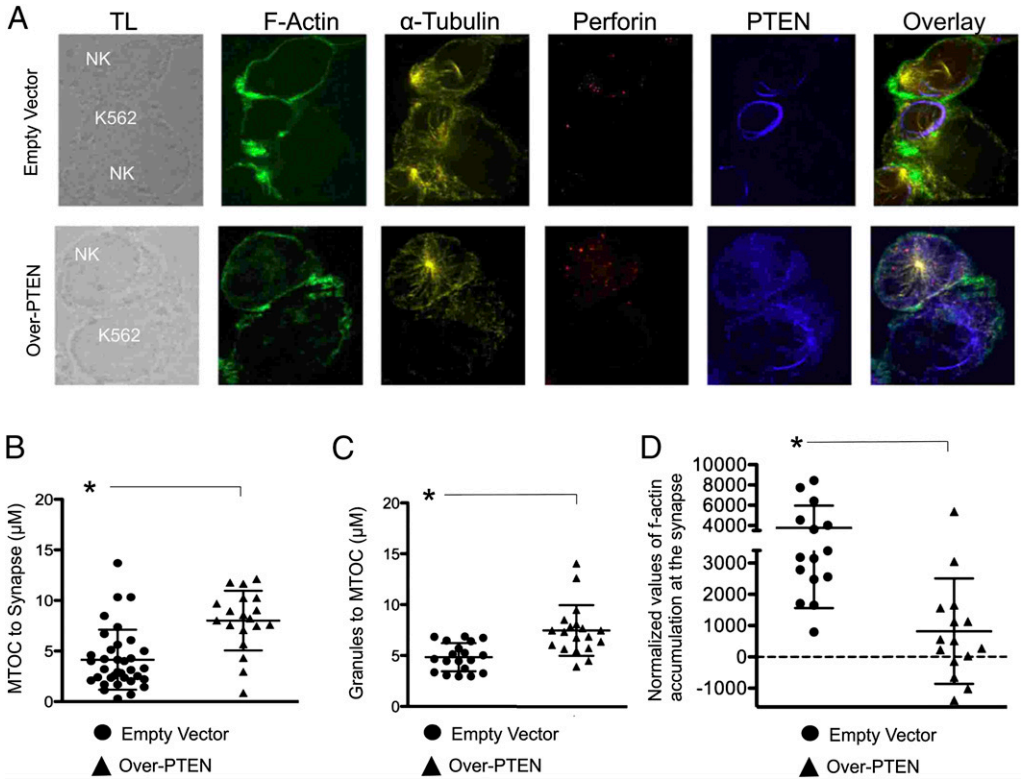

FIGURE 5. Changes in PTEN expression disrupt NK cell polarization, cytolytic granule convergence, and F-actin accumulation to the immune synapse. (**A**) Confocal representative images (original magnification ×60) of NK-92 cells (NK) infected with empty vector or Over-PTEN identified by perforin expression in immune conjugation with K562 erythroleukemia cells (K562). Shown are transmitted light (TL), single-color anti–F-actin (green), anti-tubulin (yellow), anti-perforin (red), anti-PTEN (blue), and overlay of all stains. (**B**) NK-92 cells infected with empty vector (circles) or Over-PTEN (triangles) were assessed for their ability to polarize to the target cell (measured by distance from the MTOC to the immune synapse. (**C**) NK-92 cells infected with empty vector (circles) or Over-PTEN (triangles) were assessed for the convergence of granules to the MTOC (measured the average distance of perforin containing granules to the MTOC). (**D**) NK-92 cells infected with empty vector (circles) or Over-PTEN (triangles) were assessed for the accumulation of F-actin at the immune synapse. Cells were imaged in a single *z*-plane on a Zeiss Axio-Observer Z1 equipped with a Yokogawa CSU10 spinning disc, Zeiss 63× 1.43 NA objective, and Hamamatsu Orca-AG camera. Images were acquired with Volocity software (PerkinElmer). *$p < 0.01$.

occurs during NK cell development. Forced overexpression of PTEN reduced activation of the PI3K/AKT and MAPK pathways during conjugation with malignant targets in both human and mouse NK cells and consequently reduced cytolytic activity when compared with appropriate controls. The physiologic importance of PTEN was also demonstrated by PTEN knockdown experiments in the $CD56^{bright}$ NK cell subset that showed that a decrease in PTEN protein expression led to an increase in cytolytic activity. The importance of PI3K/AKT and MAPK in the cytolytic pathway of lymphocytes has been reported (4–7) and was validated by our overexpression of PTEN with a point mutation that disabled its lipid phosphatase activity. This resulted in restoration of PI3K/AKT activation and subsequently restored NK cell cytolytic function. We also observed a failure to polarize the MTOC and a significant decrease in granule convergence at the MTOC in NK cells with overexpression of PTEN. Thus, our data suggest that PTEN normally works to limit the NK cell's PI3K/AKT and MAPK pathway activation and the consequent mobilization of cytolytic mediators toward the target cell.

Developmentally, it now appears clear that human cytolytic $CD56^{dim}$ NK cells differentiate from the less mature, noncytolytic $CD56^{bright}$ NK cells (41–45), and the current study shows that PTEN undergoes a >5-fold reduction in protein expression during this transition. Forced overexpression of PTEN in mice did not alter NK cell differentiation as determined by the quantity of immature and mature NK cell subsets and by the acquisition of NK cell activating and inhibitory receptors; however, it did prevent the phenotypically more mature NK cell subsets from acquiring optimal cytolytic activity. Thus, with a 5-fold greater expression in the $CD56^{bright}$ NK cell subset, it is possible that PTEN expression is important, along with other factors, in regulating the acquisition and the maintenance of cytolytic effector function during NK cell maturation. Our data from this study suggest one way it does that is to prevent the proper organization of the cytolytic apparatus. This may be especially relevant in the microenvironment of secondary lymphoid tissue, in which >90% of NK cells are of the $CD56^{bright}$ NK cell subset, and these cells sit within the parafollicular T cell–rich region of the tissue in direct contact with T cells and dendritic cells that produce several NK activating cytokines including IL-2, IL-12, IL-15, and IL-18 (42, 46). Other phosphatases that inhibit the PI3K/AKT pathway are expressed at lower levels in the $CD56^{bright}$ NK cell subset compared with the cytolytic $CD56^{dim}$ NK cell subset (47). Thus, abundant PTEN expression in the $CD56^{bright}$ NK cell subset may be especially important to immune homeostasis.

Our data describe a model in which elevations in PTEN expression decrease the NK cell's ability to attack tumor targets. It is conceivable that variations in PTEN expression within seemingly healthy individuals' NK cells could alter one's ability to effectively inhibit viral infection and/or malignant transformation. Indeed, an 11-y follow-up population study of 3625 people ≥40 y of age demonstrated that the potency of NK cells in peripheral blood to lyse tumor cell targets is inversely associated with cancer risk (48). Further, delayed acquisition of NK cell cytolytic function

following cancer therapy may contribute to recurrent disease (49). Perhaps most intriguing is recent evidence that PTEN can be secreted in exosomes and that the exported PTEN retains its lipid phosphatase ability upon entering the recipient cell (50). This raises the possibility that PTEN could traffic from the tumor cell target, possibly at the immune synapse, thereby immediately inhibiting NK cell activity. A similar mechanism could be potentially applied to other phosphatases with known NK cell function, including SHIP-1. Indeed, a published report has shown the presence of SHIP-1 mRNA within the exosomes of acute myeloid leukemia cell lines and primary acute myeloid leukemia patient samples (51). Whether at the mRNA or protein level, export of such molecules may offer a duel immune evasion strategy in which tumors can increase proliferation while inhibiting immune effector cell cytolytic activity. Finally, recent evidence indicates that circulating specific exogenous miRs, which are also packaged in exosomes, can modify NK cell function (52), and several miRs including miR-21, miR-26a, miR-214, miR-221, and miR-222 have each been shown to negatively regulate PTEN (36, 53–56). This creates several potential therapeutic targets for enhancing NK cell function that warrant further investigation.

Collectively, our findings demonstrate that the tumor suppressor PTEN can regulate NK cell cytolytic activity. PTEN is expressed at higher levels in the human $CD56^{bright}$ NK cell subset compared with $CD56^{dim}$ NK cells, and at high expression levels, PTEN negatively regulates NK cell cytolytic activity against a sensitive leukemia cell target. We then show that loss of PTEN in the $CD56^{bright}$ NK cell subset increases cytolytic activity. Further, mechanistically, we show that PTEN overexpression disrupts cytolytic activity through inhibition of the organization of the NK cell immune synapse, indicating that PTEN is likely an important regulator of NK cell cytolytic activity.

Disclosures

The authors have no financial conflicts of interest.

References

1. Caligiuri, M. A. 2008. Human natural killer cells. *Blood* 112: 461–469.
2. Cooper, M. A., T. A. Fehniger, and M. A. Caligiuri. 2001. The biology of human natural killer-cell subsets. *Trends Immunol.* 22: 633–640.
3. Orange, J. S. 2008. Formation and function of the lytic NK-cell immunological synapse. *Nat. Rev. Immunol.* 8: 713–725.
4. Jiang, K., B. Zhong, D. L. Gilvary, B. C. Corliss, E. Hong-Geller, S. Wei, and J. Y. Djeu. 2000. Pivotal role of phosphoinositide-3 kinase in regulation of cytotoxicity in natural killer cells. *Nat. Immunol.* 1: 419–425.
5. Chen, X., P. P. Trivedi, B. Ge, K. Krzewski, and J. L. Strominger. 2007. Many NK cell receptors activate ERK2 and JNK1 to trigger microtubule organizing center and granule polarization and cytotoxicity. *Proc. Natl. Acad. Sci. USA* 104: 6329–6334.
6. Tassi, I., M. Cella, S. Gilfillan, I. Turnbull, T. G. Diacovo, J. M. Penninger, and M. Colonna. 2007. p110gamma and p110delta phosphoinositide 3-kinase signaling pathways synergize to control development and functions of murine NK cells. *Immunity* 27: 214–227.
7. Trotta, R., K. A. Puorro, M. Paroli, L. Azzoni, B. Abebe, L. C. Eisenlohr, and B. Perussia. 1998. Dependence of both spontaneous and antibody-dependent, granule exocytosis-mediated NK cell cytotoxicity on extracellular signal-regulated kinases. *J. Immunol.* 161: 6648–6656.
8. Liu, S., H. Zhang, M. Li, D. Hu, C. Li, B. Ge, B. Jin, and Z. Fan. 2013. Recruitment of Grb2 and SHIP1 by the ITT-like motif of TIGIT suppresses granule polarization and cytotoxicity of NK cells. *Cell Death Differ.* 20: 456–464.
9. Chalhoub, N., and S. J. Baker. 2009. PTEN and the PI3-kinase pathway in cancer. *Annu. Rev. Pathol.* 4: 127–150.
10. Eng, C. 2003. PTEN: one gene, many syndromes. *Hum. Mutat.* 22: 183–198.
11. Chen, Z., L. C. Trotman, D. Shaffer, H. K. Lin, Z. A. Dotan, M. Niki, J. A. Koutcher, H. I. Scher, T. Ludwig, W. Gerald, et al. 2005. Crucial role of p53-dependent cellular senescence in suppression of Pten-deficient tumorigenesis. *Nature* 436: 725–730.
12. Funamoto, S., R. Meili, S. Lee, L. Parry, and R. A. Firtel. 2002. Spatial and temporal regulation of 3-phosphoinositides by PI 3-kinase and PTEN mediates chemotaxis. *Cell* 109: 611–623.
13. Liliental, J., S. Y. Moon, R. Lesche, R. Mamillapalli, D. Li, Y. Zheng, H. Sun, and H. Wu. 2000. Genetic deletion of the Pten tumor suppressor gene promotes cell motility by activation of Rac1 and Cdc42 GTPases. *Curr. Biol.* 10: 401–404.
14. Tamura, M., J. Gu, K. Matsumoto, S. Aota, R. Parsons, and K. M. Yamada. 1998. Inhibition of cell migration, spreading, and focal adhesions by tumor suppressor PTEN. *Science* 280: 1614–1617.
15. Martin-Belmonte, F., A. Gassama, A. Datta, W. Yu, U. Rescher, V. Gerke, and K. Mostov. 2007. PTEN-mediated apical segregation of phosphoinositides controls epithelial morphogenesis through Cdc42. *Cell* 128: 383–397.
16. Raftopoulou, M., S. Etienne-Manneville, A. Self, S. Nicholls, and A. Hall. 2004. Regulation of cell migration by the C2 domain of the tumor suppressor PTEN. *Science* 303: 1179–1181.
17. Trimboli, A. J., C. Z. Cantemir-Stone, F. Li, J. A. Wallace, A. Merchant, N. Creasap, J. C. Thompson, E. Caserta, H. Wang, J. L. Chong, et al. 2009. Pten in stromal fibroblasts suppresses mammary epithelial tumours. *Nature* 461: 1084–1091.
18. Bronisz, A., J. Godlewski, J. A. Wallace, A. S. Merchant, M. O. Nowicki, H. Mathsyaraja, R. Srinivasan, A. J. Trimboli, C. K. Martin, F. Li, et al. 2012. Reprogramming of the tumour microenvironment by stromal PTEN-regulated miR-320. *Nat. Cell Biol.* 14: 159–167.
19. Shen, W. H., A. S. Balajee, J. Wang, H. Wu, C. Eng, P. P. Pandolfi, and Y. Yin. 2007. Essential role for nuclear PTEN in maintaining chromosomal integrity. *Cell* 128: 157–170.
20. Puc, J., M. Keniry, H. S. Li, T. K. Pandita, A. D. Choudhury, L. Memeo, M. Mansukhani, V. V. Murty, Z. Gaciong, S. E. Meek, et al. 2005. Lack of PTEN sequesters CHK1 and initiates genetic instability. *Cancer Cell* 7: 193–204.
21. Suzuki, A., M. T. Yamaguchi, T. Ohteki, T. Sasaki, T. Kaisho, Y. Kimura, R. Yoshida, A. Wakeham, T. Higuchi, M. Fukumoto, et al. 2001. T cell-specific loss of Pten leads to defects in central and peripheral tolerance. *Immunity* 14: 523–534.
22. Soond, D. R., F. Garçon, D. T. Patton, J. Rolf, M. Turner, C. Scudamore, O. A. Garden, and K. Okkenhaug. 2012. Pten loss in CD4 T cells enhances their helper function but does not lead to autoimmunity or lymphoma. *J. Immunol.* 188: 5935–5943.
23. Walsh, P. T., J. L. Buckler, J. Zhang, A. E. Gelman, N. M. Dalton, D. K. Taylor, S. J. Bensinger, W. W. Hancock, and L. A. Turka. 2006. PTEN inhibits IL-2 receptor-mediated expansion of CD4+ CD25+ Tregs. *J. Clin. Invest.* 116: 2521–2531.
24. Haxhinasto, S., D. Mathis, and C. Benoist. 2008. The AKT-mTOR axis regulates de novo differentiation of CD4+Foxp3+ cells. *J. Exp. Med.* 205: 565–574.
25. Sauer, S., L. Bruno, A. Hertweck, D. Finlay, M. Leleu, M. Spivakov, Z. A. Knight, B. S. Cobb, D. Cantrell, E. O'Connor, et al. 2008. T cell receptor signaling controls Foxp3 expression via PI3K, Akt, and mTOR. *Proc. Natl. Acad. Sci. USA* 105: 7797–7802.
26. Kishimoto, H., T. Ohteki, N. Yajima, K. Kawahara, M. Natsui, S. Kawarasaki, K. Hamada, Y. Horie, Y. Kubo, S. Arase, et al. 2007. The Pten/PI3K pathway governs the homeostasis of Valpha14iNKT cells. *Blood* 109: 3316–3324.
27. Trotta, R., L. Chen, D. Ciarlariello, S. Josyula, C. Mao, S. Costinean, L. Yu, J. P. Butchar, S. Tridandapani, C. M. Croce, and M. A. Caligiuri. 2012. miR-155 regulates IFN-γ production in natural killer cells. *Blood* 119: 3478–3485.
28. Trotta, R., L. Chen, S. Costinean, S. Josyula, B. L. Mundy-Bosse, D. Ciarlariello, C. Mao, E. L. Briercheck, K. K. McConnell, A. Mishra, et al. 2013. Overexpression of miR-155 causes expansion, arrest in terminal differentiation and functional activation of mouse natural killer cells. *Blood* 121: 3126–3134.
29. Trotta, R., T. Vignudelli, O. Candini, R. V. Intine, L. Pecorari, C. Guerzoni, G. Santilli, M. W. Byrom, S. Goldoni, L. P. Ford, et al. 2003. BCR/ABL activates mdm2 mRNA translation via the La antigen. *Cancer Cell* 3: 145–160.
30. Sanborn, K. B., G. D. Rak, S. Y. Maru, K. Demers, A. Difeo, J. A. Martignetti, M. R. Betts, R. Favier, P. P. Banerjee, and J. S. Orange. 2009. Myosin IIA associates with NK cell lytic granules to enable their interaction with F-actin and function at the immunological synapse. *J. Immunol.* 182: 6969–6984.
31. Garcia-Cao, I., M. S. Song, R. M. Hobbs, G. Laurent, C. Giorgi, V. C. de Boer, D. Anastasiou, K. Ito, A. T. Sasaki, L. Rameh, et al. 2012. Systemic elevation of PTEN induces a tumor-suppressive metabolic state. *Cell* 149: 49–62.
32. Kim, J. S., X. Xu, H. Li, D. Solomon, W. S. Lane, T. Jin, and T. Waldman. 2011. Mechanistic analysis of a DNA damage-induced, PTEN-dependent size checkpoint in human cells. *Mol. Cell. Biol.* 31: 2756–2771.
33. Banerjee, P. P., R. Pandey, R. Zheng, M. M. Suhoski, L. Monaco-Shawver, and J. S. Orange. 2007. Cdc42-interacting protein-4 functionally links actin and microtubule networks at the cytolytic NK cell immunological synapse. *J. Exp. Med.* 204: 2305–2320.
34. Mentlik, A. N., K. B. Sanborn, E. L. Holzbaur, and J. S. Orange. 2010. Rapid lytic granule convergence to the MTOC in natural killer cells is dependent on dynein but not cytolytic commitment. *Mol. Biol. Cell* 21: 2241–2256.
35. Holm, S. 1979. A simple sequentially rejective multiple test procedure. *Scand. J. Statist.* 6: 65–70.
36. Huse, J. T., C. Brennan, D. Hambardzumyan, B. Wee, J. Pena, S. H. Rouhanifard, C. Sohn-Lee, C. le Sage, R. Agami, T. Tuschl, and E. C. Holland. 2009. The PTEN-regulating microRNA miR-26a is amplified in high-grade glioma and facilitates gliomagenesis in vivo. *Genes Dev.* 23: 1327–1337.
37. Chiossone, L., J. Chaix, N. Fuseri, C. Roth, E. Vivier, and T. Walzer. 2009. Maturation of mouse NK cells is a 4-stage developmental program. *Blood* 113: 5488–5496.
38. Hayakawa, Y., and M. J. Smyth. 2006. CD27 dissects mature NK cells into two subsets with distinct responsiveness and migratory capacity. *J. Immunol.* 176: 1517–1524.

39. Stambolic, V., A. Suzuki, J. L. de la Pompa, G. M. Brothers, C. Mirtsos, T. Sasaki, J. Ruland, J. M. Penninger, D. P. Siderovski, and T. W. Mak. 1998. Negative regulation of PKB/Akt-dependent cell survival by the tumor suppressor PTEN. *Cell* 95: 29–39.
40. Gumbleton, M., and W. G. Kerr. 2013. Role of inositol phospholipid signaling in natural killer cell biology. *Front. Immunol.* 4: 47.
41. Freud, A. G., and M. A. Caligiuri. 2006. Human natural killer cell development. *Immunol. Rev.* 214: 56–72.
42. Freud, A. G., A. Yokohama, B. Becknell, M. T. Lee, H. C. Mao, A. K. Ferketich, and M. A. Caligiuri. 2006. Evidence for discrete stages of human natural killer cell differentiation in vivo. *J. Exp. Med.* 203: 1033–1043.
43. Yu, J., H. C. Mao, M. Wei, T. Hughes, J. Zhang, I. K. Park, S. Liu, S. McClory, G. Marcucci, R. Trotta, and M. A. Caligiuri. 2010. CD94 surface density identifies a functional intermediary between the CD56bright and CD56dim human NK-cell subsets. *Blood* 115: 274–281.
44. Della Chiesa, M., M. Falco, M. Podestà, F. Locatelli, L. Moretta, F. Frassoni, and A. Moretta. 2012. Phenotypic and functional heterogeneity of human NK cells developing after umbilical cord blood transplantation: a role for human cytomegalovirus? *Blood* 119: 399–410.
45. Lopez-Vergès, S., J. M. Milush, S. Pandey, V. A. York, J. Arakawa-Hoyt, H. Pircher, P. J. Norris, D. F. Nixon, and L. L. Lanier. 2010. CD57 defines a functionally distinct population of mature NK cells in the human CD56dimCD16+ NK-cell subset. *Blood* 116: 3865–3874.
46. Fehniger, T. A., M. H. Shah, M. J. Turner, J. B. VanDeusen, S. P. Whitman, M. A. Cooper, K. Suzuki, M. Wechser, F. Goodsaid, and M. A. Caligiuri. 1999. Differential cytokine and chemokine gene expression by human NK cells following activation with IL-18 or IL-15 in combination with IL-12: implications for the innate immune response. *J. Immunol.* 162: 4511–4520.
47. Trotta, R., R. Parihar, J. Yu, B. Becknell, J. Allard, II, J. Wen, W. Ding, H. Mao, S. Tridandapani, W. E. Carson, and M. A. Caligiuri. 2005. Differential expression of SHIP1 in CD56bright and CD56dim NK cells provides a molecular basis for distinct functional responses to monokine costimulation. *Blood* 105: 3011–3018.
48. Imai, K., S. Matsuyama, S. Miyake, K. Suga, and K. Nakachi. 2000. Natural cytotoxic activity of peripheral-blood lymphocytes and cancer incidence: an 11-year follow-up study of a general population. *Lancet* 356: 1795–1799.
49. Markasz, L., G. Stuber, B. Vanherberghen, E. Flaberg, E. Olah, E. Carbone, S. Eksborg, E. Klein, H. Skribek, and L. Szekely. 2007. Effect of frequently used chemotherapeutic drugs on the cytotoxic activity of human natural killer cells. *Mol. Cancer Ther.* 6: 644–654.
50. Putz, U., J. Howitt, A. Doan, C. P. Goh, L. H. Low, J. Silke, and S. S. Tan. 2012. The tumor suppressor PTEN is exported in exosomes and has phosphatase activity in recipient cells. *Sci. Signal.* 5: ra70.
51. Huan, J., N. I. Hornick, M. J. Shurtleff, A. M. Skinner, N. A. Goloviznina, C. T. Roberts, Jr., and P. Kurre. 2013. RNA trafficking by acute myelogenous leukemia exosomes. *Cancer Res.* 73: 918–929.
52. He, S., J. Chu, L. C. Wu, H. Mao, Y. Peng, C. A. Alvarez-Breckenridge, T. Hughes, M. Wei, J. Zhang, S. Yuan, et al. 2013. MicroRNAs activate natural killer cells through Toll-like receptor signaling. *Blood* 121: 4663–4671.
53. Chun-Zhi, Z., H. Lei, Z. An-Ling, F. Yan-Chao, Y. Xiao, W. Guang-Xiu, J. Zhi-Fan, P. Pei-Yu, Z. Qing-Yu, and K. Chun-Sheng. 2010. MicroRNA-221 and microRNA-222 regulate gastric carcinoma cell proliferation and radioresistance by targeting PTEN. *BMC Cancer* 10: 367.
54. Xie, Q., Y. Yan, Z. Huang, X. Zhong, and L. Huang. 2014. MicroRNA-221 targeting PI3-K/Akt signaling axis induces cell proliferation and BCNU resistance in human glioblastoma. *Neuropathology* 34: 455–464.
55. Meng, F., R. Henson, H. Wehbe-Janek, K. Ghoshal, S. T. Jacob, and T. Patel. 2007. MicroRNA-21 regulates expression of the PTEN tumor suppressor gene in human hepatocellular cancer. *Gastroenterology* 133: 647–658.
56. Yang, H., W. Kong, L. He, J. J. Zhao, J. D. O'Donnell, J. Wang, R. M. Wenham, D. Coppola, P. A. Kruk, S. V. Nicosia, and J. Q. Cheng. 2008. MicroRNA expression profiling in human ovarian cancer: miR-214 induces cell survival and cisplatin resistance by targeting PTEN. *Cancer Res.* 68: 425–433.